2016 IEEE/RSJ International Conference on Intelligent Robots and Systems (IROS)
Daejeon Convention Center
October 9-14, 2016, Daejeon, Korea

# Towards Multi-Modal Intention Interfaces for Human-Robot Co-Manipulation

Luka Peternel, Nikos Tsagarakis and Arash Ajoudani

***Abstract*— This paper presents a novel approach for human-robot cooperation in tasks with dynamic uncertainties. The essential element of the proposed method is a multi-modal interface that provides the robot with the feedback about the human motor behaviour in real-time. The human muscle activity measurements and the arm force manipulability properties encode the information about the motion and impedance, and the intended configuration of the task frame, respectively. Through this human-in-the-loop framework, the developed hybrid controller of the robot can adapt its actions to provide the desired motion and impedance regulation in different phases of the cooperative task. We experimentally evaluate the proposed approach in a two-person sawing task that requires an appropriate complementary behaviour from the two agents.**

## I. Introduction

Physical human-robot interaction and cooperation are two fundamental and necessary aspects for integrating robots into our daily lives. The robots are expected to help us in various tasks, of which many require collaborative effort to be successfully completed. In order to achieve such behaviour, the robot must be able to physically interact with the human counterpart and predict the intentions[1] of the human, despite the additional interaction with the uncertain and unpredictable environment.

To partially address the problem of physical interaction with an unstructured and unpredictable environment, the impedance control approach was introduced that facilitates indirect regulations of the interaction forces in contact [1], [2]. This is achieved by the implementation of a mass-spring-damper system with a desired dynamic response. In simple cases, the parameters of such a system can be identified in advance and kept fixed throughout the task execution. However, in cases where the environment or the task interaction forces are a subject to variations or uncertainties, the desired response must be adaptively regulated though the impedance parameters and the reference motion, force, task frame, frequency etc. [3]–[10]. This aspect is particularly important in the human-robot cooperation scenarios, which demand that the robot actively reads the intention of the human counterpart and reacts accordingly.

The intention of the human can be transferred to the robot through different modalities and interfaces. For instance, force sensing can be used on the robot side to read the objective of the human partner and/or control the cooperation effort. Some examples include: collaborative object transportation [11]–[17], object lifting [18], object placing [5], [14], object swinging [19], [20] and posture assistance [21], [22]. Nevertheless, collaborative tasks that involve simultaneous interaction with a rough environment (e.g. co-manipulative tool-use) can induce various unpredictable force components to the force sensor reading [6]. In this case, it can be difficult to distinguish the components related to the human behaviour from the ones generated from the interaction with the environment. Alternatively, visual feedback [16], [23] or language commands [24] can be used to determine the human intention and generate the desired trajectory for the robot controller. However, in some cases the task complexity could potentially prevent the robot from deriving the desired sensorimotor behaviour from these higher level feedback modalities.

Another option to obtain the desired collaborative robot behaviour directly on a sensorimotor level is to use robot learning techniques such as: gradual mutual adaptation [21], [25], reinforcement learning [20] or human demonstration [6], [8], [17], [18], [22], [26], [27]. In this direction, the tele-impedance principle[2] was used in a robot learning approach [6], where the demonstrator could teach the robotic arm how to cooperate with a human partner for co-manipulative tool-

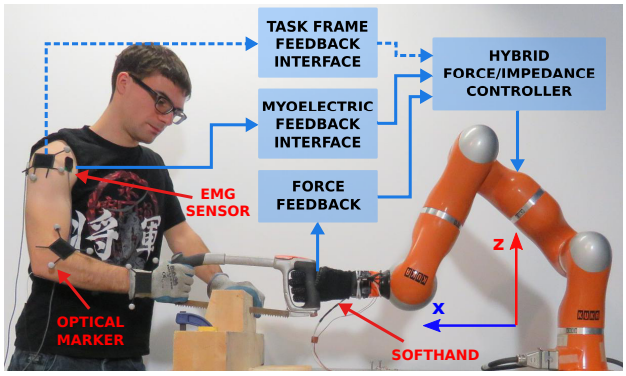


Fig. 1: Human-robot cooperation framework for co-manipulative tasks. The robot is controlled by a hybrid force/impedance controller. The myoelectric feedback interface provides the robot controller with human motor behaviour feedback for position related tasks. Additional task-frame configuration feedback is based on estimating the force manipulability ellipsoid. This interface provides the robot controller with feedback about the desired configuration of the task frame. Force/torque sensors provide a feedback for force/torque related tasks. Orientation of robot base frame is shown by red and blue arrows.

Authors are with HRI[2] Lab and HHCM Lab, Department of Advanced Robotics, Istituto Italiano di Tecnologia, Genoa, Italy, Email: luka.peternel@iit.it

This work was supported in part by the H2020 project CogIMon (ICT-23-2014, 644727).

[1]Intention is the current objective and task, not future state estimation.

[2]Tele-impedance is an enhanced version of the teleoperation where the robot's Cartesian impedance can be regulated using enriched command channel from the operator [4].



Authorized licensed use limited to: Xian Jiaotong University. Downloaded on January 21,2021 at 09:30:29 UTC from IEEE Xplore. Restrictions apply.

use. In this approach the demonstrator was teleoperating the robotic arm and controlling its motion and stiffness trajectories, while cooperating with the human. The learnt trajectories were then used by the robot in the autonomous stage in a periodic manner. The execution speed of the robot was adapted by a feedback based on the estimated human partner motion through an adaptive oscillator. This approach can be effective to solve cooperative human-robot co-manipulation, however it requires relatively complex setup and an experienced demonstrator to achieve a good performance.

In this paper, we propose a new method for intuitive human-robot co-manipulation that is based on reading the intention directly from the limb function/properties of the cooperating human partner. With this, we bypass the above-mentioned problems related to the human intention estimation from the force sensor reading on the robot side. Instead of using complex learning-by-demonstration techniques [6], [8], [17], [26], [27], we rely on a minimal degree of pre-programming. The approach is based on a hybrid force/impedance control scheme, where we can determine which axes should be used for indirect (through motion) and direct force regulation tasks. To extract the human intention and feed it to the robot, we developed a multi-modal human-robot interface that incorporates human muscular activities and arm configuration feedback. The myoelectric feedback is used to estimate the human arm stiffness trend that is directly used in the robot impedance control, while the frame of the task is adjusted based on the estimated force manipulability ellipsoid of the human arm endpoint.

The proposed approach offers a high degree of adaptability in a sense that the human can perform the task at an arbitrary pace. Unlike in [6], this is done without an additional frequency estimation system. The human can also stop and continue the execution at any time, while the robot reacts actively and accordingly. In addition, the task-frame configuration feedback interface allows the human to reconfigure the task frame in which the cooperative task is executed. Based on this feedback, the robot simply rotates the task frame in Cartesian space to follow the human intention, while the definition of the task in a sense of designated impedance/force axes remains unchanged. Therefore, the proposed approach establishes a shared authority framework where the human controls the cognitive aspects of the task while the robot provides the assistance on the motor level.

We validate the proposed approach with experiments on a real system using KUKA Lightweight Robot equipped with the Pisa/IIT Softhand (see Fig. 1). The cooperative woodcutting with a two-person crosscut saw was selected as the experimental task as it requires an appropriate and strict coordination between the agents. Moreover, the execution of this task requires a rough and unpredictable interaction with the environment. These challenging aspects of the selected task provide a demanding real world evaluation experiment for the proposed approach.

## II. METHOD

The block scheme of the proposed framework is shown in Fig. 1. The framework is composed of four main units: (1) hybrid force/impedance controller, (2) force feedback unit that provides the necessary feedback for force related tasks, (3) myoelectric feedback interface that provides the primary feedback about the human behaviour and (4) task-frame configuration interface that provides the feedback about the human-intended task frame configuration.

### A. Hybrid Force/Impedance Controller

The hybrid force/impedance control scheme has demonstrated its advantage over pure force or impedance control techniques while interacting with an unknown environment [9], [10]. The main advantage of this control scheme is that the robotic platform can regulate force and impedance in certain Cartesian directions required by the task. Therefore, we adopt the hybrid force/impedance control scheme into our approach to establish a desired force between the tool and the environment (through direct force axes), and being able to address the environmental uncertainties while executing the task (through impedance axes). As regards the sawing task, the desired interaction force/torque in the task reference frame is defined by

$$\boldsymbol{F}_{int} = \boldsymbol{F}_{force} + \boldsymbol{K}\left(\boldsymbol{x}_a - \boldsymbol{x}_d\right) + \boldsymbol{D}\left(\dot{\boldsymbol{x}}_a - \dot{\boldsymbol{x}}_d\right), \tag{1}$$

where $\boldsymbol{F}_{int}$ is the Cartesian space interaction force/torque acting from the environment on the robot, $\boldsymbol{K}$ and $\boldsymbol{D}$ are robot virtual stiffness and damping matrices in Cartesian space, $\boldsymbol{x}_a$ is actual and $\boldsymbol{x}_d$ is reference pose of the robot end-effector. The term $\boldsymbol{F}_{force}$ is related to the force task, i.e. force control in certain axes, and is meant to ensure the contact between the tool and the environment in those directions. $\boldsymbol{F}_{force}$ was controlled by a PI controller[3] based on the measured/estimated force feedback

$$\boldsymbol{F}_{force} = \boldsymbol{K}_P^F \boldsymbol{e}_F + \boldsymbol{K}_I^F \int \boldsymbol{e}_F \mathrm{d}t, \tag{2}$$

$$\boldsymbol{e}_F = \boldsymbol{S}_F\left(\boldsymbol{F}_a - \boldsymbol{F}_d\right), \tag{3}$$

where $\boldsymbol{e}_F$ is the error between the actual force $\boldsymbol{F}_a$ and desired force $\boldsymbol{F}_d$, $\boldsymbol{K}^F$ are gains of PI controller and $\boldsymbol{S}_F$ is a diagonal matrix that is used to select the axes in which the force should be controlled. If the axis is force controlled, the respective diagonal element should be equal to one; otherwise it is set to zero. PI controller was used to compensate for uncertainties such as: environmental disturbances, model and kinematics errors, joint friction, etc.

The desired interaction force $\boldsymbol{F}_{int}$ in Cartesian space was controlled at the robot joint torque level

$$\boldsymbol{M}(\boldsymbol{q})\ddot{\boldsymbol{q}} + \boldsymbol{C}(\boldsymbol{q},\dot{\boldsymbol{q}})\dot{\boldsymbol{q}} + \boldsymbol{g}(\boldsymbol{q}) = \boldsymbol{\tau} + \boldsymbol{J}_r^T \boldsymbol{F}_{int}, \tag{4}$$

where $\boldsymbol{\tau}$ is a vector of robot joint torques, $\boldsymbol{q}$ is vector of joint angles, $\boldsymbol{J}_r$ is robot arm Jacobian matrix, $\boldsymbol{M}$ is mass matrix, $\boldsymbol{C}$ is Coriolis and centrifugal vector and $\boldsymbol{g}$ is gravity vector.

[3]Derivative term was not used to avoid stability issues as the force measurement is noisy due to the rough interaction with the environment.



Authorized licensed use limited to: Xian Jiaotong University. Downloaded on January 21,2021 at 09:30:29 UTC from IEEE Xplore. Restrictions apply.

Given that we know the dynamical model of the robot, we can calculate the necessary joint torques $\boldsymbol{\tau}$ to produce the desired interaction force/torque $\boldsymbol{F}_{int}$. The calculated torques $\boldsymbol{\tau}$ were used to control KUKA robotic arm in joint torque control mode.

### B. Myoelectic Feedback Interface

As mentioned earlier, this feedback was meant to enable the robot to replicate an appropriate stiffness increasing/decreasing regulation strategy in our human-robot co-manipulation setup. Indeed, phase-dependent stiffness increasing/decreasing regulation strategy of the human partners in cooperative tasks has been shown to play a very important role in the determination and perception of the leader-follower roles [6], [28]. Towards this objective, one can exploit a complex model of the human arm endpoint stiffness (see [4], [29]) to achieve the volume and the direction (task-frame) of the desired Cartesian stiffness profile. This process requires an off-line identification and calibration phase that will certainly limit the application of the proposed setup, especially in household or industrial settings. In this paper, we break down this problem by tracking the stiffening trend of the human operator using a simplistic approach, while the intended task frame is identified using a more practical method as explained in section II-C.

Electromyography (EMG) signals of muscles were measured using Delsys Bagnoli Desktop EMG system. Rectified and filtered EMG was then normalised using maximal voluntary contraction (MVC). The mapping between the processed EMG and muscle activation level was defined as

$$0 \leq A_i(t) = \frac{EMG_i(t)}{MVC_i} \leq 1, \tag{5}$$

where $A$ is muscle activation level, $EMG(t)$ is processed EMG signal and $MVC$ is EMG signal under maximal voluntary contraction of the muscle. Subscript number $i$ corresponds to agonist and antagonist muscles of the chosen muscle pair.

The mapping between the muscle activation and joint stiffness trend ($c_h$) was defined as [30]

$$c_h = b_1 \frac{1 - e^{-b_2(A_1+A_2)}}{1 + e^{-b_2(A_1+A_2)}}, \tag{6}$$

where parameter $b_1$ defines maximum amplitude and $b_2$ defines the shape, and are determined experimentally. The stiffness estimation can be scaled $c'_h = a \cdot c_h$ to a certain operational range of the human stiffness, where factor $a$ is determined experimentally (see section III). Condition $c'_h \in [0,1]$ and $c_h \in [0,1]$ should be maintained.

We used a simplified single joint stiffness as an estimation of the human arm stiffness in the relevant axis of Cartesian space [29]. Antagonistic muscle measurements allow for detection of pulling, pushing and co-contraction actions. In our case, we selected shoulder stiffness that has a dominant role in controlling the endpoint stiffness in this specific task. Nonetheless, it is well-known that such a pattern can be observed in other antagonistic pairs since human arm muscle activations follow a synergistic pattern [31], [32].

The mapping between the estimated human stiffness and robotic arm stiffness modulation parameter was defined as

$$k_r = c'_h(k_{max} - k_{min}) + k_{min}, \tag{7}$$

where $k_{max}$ and $k_{min}$ determine the range of controllable robot stiffness.

*1) Reciprocal Tele-Impedance:* If the task is reciprocal in terms of phase of operation, the robot should read the human intention and behave in a reciprocal manner. An example of such task is cooperative sawing. While the human operator is stiff to pull the saw, the robot must remain compliant not to oppose the effort of the first agent. In the next phase the roles are reversed and the robot becomes stiff to pull the saw, while the human reduces the stiffness and remains compliant. The stiffness in axis/axes designated for motion (through impedance control) was obtained by

$$\boldsymbol{K}_{ctrl} = \boldsymbol{S}_K\big(1 - k_r\big), \tag{8}$$

where $\boldsymbol{S}_K$ is a diagonal matrix that is used to select the axes in which the stiffness should be modulated (units of the first three elements are N/m, while the last three are Nm/rad) and $\boldsymbol{K}_{ctrl}$ is matrix that is used to control the stiffness of the designated axes. If the specific axis should be constant then the respective diagonal element of $\boldsymbol{S}_K$ should be equal zero. The robot Cartesian stiffness used in (1) is equal to

$$\boldsymbol{K} = \boldsymbol{K}_{const} + \boldsymbol{K}_{ctrl}, \tag{9}$$

where $\boldsymbol{K}_{const}$ is a diagonal matrix containing stiffness values of axes that should be constant.

*2) Mirrored Tele-Impedance:* If the task requires both agents to produce the same behaviour in a certain phase of task operation, the human intention should be mirrored on the robot side. One such example is cooperative bolt screwing or valve turning. When the bolt/valve should be turned, both agents should be stiff to produce torque in the same direction and perform the rotation. In the next phase, both agents should become complaint to reconfigure and prepare for another rotation cycle. In such case, the human stiffness should be mirrored on the robot as

$$\boldsymbol{K}_{ctrl} = \boldsymbol{S}_K k_r, \tag{10}$$

where $\boldsymbol{K}_{ctrl}$ can be used in (9).

### C. Task-Frame Configuration Feedback Interface

It is well known that humans exploit arm configurations to achieve a task-appropriate kinematic or dynamic behaviour. In particular, some postures are more efficient for producing a given task. Therefore, one basic way to understand the intention of the human cooperator is to observe the pose-related properties, such as velocity and force manipulability measures. For example in the sawing task, the sawing motion axis requires a force production to pull the saw and drive the blade, which in turn cuts the material. Ideally, the human should align the sawing axis with the highest force manipulability direction to optimise that task execution. The robot should then adjust its own sawing motion axis to follow the human intention and accommodate the collaborative effort.



Authorized licensed use limited to: Xian Jiaotong University. Downloaded on January 21,2021 at 09:30:29 UTC from IEEE Xplore. Restrictions apply.

In the proposed approach the robot task reference frame is adjusted based on the estimated human arm endpoint force manipulability ellipsoid. This measure describes the major directions in which the human operator can effectively control the interaction forces. The force manipulability can be derived from

$$\boldsymbol{\tau} = \boldsymbol{J}_h^T \boldsymbol{F}, \quad \boldsymbol{\tau}^T \boldsymbol{\tau} = 1, \quad \boldsymbol{F}^T \boldsymbol{J}_h \boldsymbol{J}_h^T \boldsymbol{F} = 1, \tag{11}$$

where $\boldsymbol{J}_h$ is human arm Jacobian matrix, $\boldsymbol{\tau}$ is joint torque vector and $\boldsymbol{F}$ is endpoint force vector.

The endpoint force manipulability ellipsoid can be determined by eigenvalues and eigenvectors of $(\boldsymbol{J}_h \boldsymbol{J}_h^T)^{-1}$. We used eigenvectors to determine the orientation of the task frame in a way that the dominant axis of the force manipulability ellipsoid was aligned with the sawing axis. The adjusted stiffness matrix $\boldsymbol{K}_{adj}$ in the robot base frame was therefore obtained by

$$\boldsymbol{K}_{adj} = \boldsymbol{U}_R \cdot \boldsymbol{K}_{eig} \cdot \boldsymbol{V}_R^T, \tag{12}$$

where $\boldsymbol{K}_{eig}$ is a diagonal matrix containing eigenvalues of stiffness matrix $\boldsymbol{K}$. Matrices $\boldsymbol{U}_R$ and $\boldsymbol{V}_R$ contain left and right eigenvectors and were obtained by singular value decomposition of $(\boldsymbol{J}_h \boldsymbol{J}_h^T)^{-1}$. In addition to adjusting the stiffness matrix, we also controlled the orientation of the robotic hand to align it with the task frame and match to the orientation of the human hand.

We based our Cartesian damping approach on *factorisation design* [33].[4] The damping matrix $\boldsymbol{D}$ was calculated based on the adjusted Cartesian stiffness matrix

$$\boldsymbol{D} = \boldsymbol{\Lambda}_* \boldsymbol{D}_\xi \boldsymbol{K}_{adj*} + \boldsymbol{K}_{adj*} \boldsymbol{D}_\xi \boldsymbol{\Lambda}_*, \tag{13}$$

where $\boldsymbol{D}_\xi$ is a diagonal matrix containing the damping factors ($\xi = 0.7$), $\boldsymbol{K}_{adj*} \boldsymbol{K}_{adj*} = \boldsymbol{K}_{adj}$ and $\boldsymbol{\Lambda}_* \boldsymbol{\Lambda}_* = \boldsymbol{\Lambda}$, where $\boldsymbol{\Lambda}$ is the Cartesian inertia matrix of the KUKA robot.

## III. Experiments

To validate the proposed approach we designed an experiment where the task of the cooperative partners was using two-person saw to cut a beam of wood. This task requires a good coordination between the human and the robot. Generally, a preferable strategy is to split the task in two phases. In the *first phase* the human has to pull/push the saw along the blade to dive the saw, while the cooperating robot should stay compliant in the motion axis in order not to oppose the human's effort. Simultaneously, both human and robot should apply some vertical downward force to produce the friction between the saw teeth and the material. When the saw blade reaches the edge, the roles are switched. In the *second phase*, the robot starts to pull/push the saw back toward itself, while the human stays compliant in the motion axis in order not to oppose robot's effort.

The robot's hybrid controller achieved a Cartesian impedance profile along the direction of the sawing motion ($x-y$ plane). The maximum controllable stiffness along the primary motion axis was set to $k_{max} = 1000$ N/m. The minimum robot stiffness was set to $k_{min} = 100$ N/m to mimic the passive stiffness in human muscles. The robot end-effector reference position in this axis was predetermined at the point where the saw blade is at the edge on the robot side. In this way, the robot moved the saw to the desired end position in the phase when it was its turn to pull. When the human pulled back, the robot became compliant and allowed the human to move the saw blade to the other edge by permitting to displace the actual position from the preset desired position. The stiffness in axis perpendicular to the primary motion axis in horizontal plane was set to 0 N/m. This allowed the free motion along that axis and provided the human the adaptability to make a cut at any point along the beam. The rotational stiffness was kept constant at a relatively high vale $k_{rot} = 250$ Nm/rad in all axes in order to maintain the desired rotational posture.

To ensure the contact between the blade and the wood, the robot produced a force in vertical axis according to the PI controller described by (2). We experimentally set the proportional gains of controller in z-axis to 0.5 and integral gains to 1.0. The desired force in z-axis was set to $F_d = -5$ N.

The selected task requires the agents to produce reciprocal actions in any of the phases. To control the robot stiffness we used the proposed interface based on human muscle activity biofeedback described by (7)-(9). For this task, we selected human shoulder joint Deltoid muscle activity to estimate the robot arm stiffness properties. The surface EMG electrodes were placed on Posterior Deltoid and Anterior Deltoid muscles. Before the experiment, we performed a MVC procedure for both selected muscles and used the obtained values in EMG normalisation. We set $b_1 = 20$ and $b_2 = 0.05$ experimentally. Factor $a = 12$ was set experimentally based on a preliminary human-human collaboration trials. Factor $a$ was obtained by an inverse value of average minimum peak of the measured $c_h$ signal.

In the first part of the experiment we demonstrated cooperative task execution between the human and robot counterparts.The results are shown in Fig. 2. Please refer to supplementary multimedia file for a video of the experiment. The first graph shows the estimated human stiffness parameter $c_h$, while the second graph shows the robot stiffness along the sawing motion axis. The two are reciprocal according to (7). When the human was pulling the saw, the human stiffness increased and the robot stiffness decreased in order to follow the human action. When the human stopped pulling, the robot stiffness increased and consequently the robot began to pull the saw back toward itself. The motion of the robot end-effector along the sawing axis (in this case aligned with robot base frame x-axis) can be confirmed in the third graph. While the human and robot cooperatively executed the given task, the wood was gradually cut and the vertical robot end-effector position gradually moved downward, as it can be confirmed by measurements in the third graph.

The fourth graph shows the robot force in vertical axis, which is necessary to maintain the contact between the

[4] Alternatively, the damping approach can be based on *double diagonalisation design* [33] while similarily using $K_{adj}$ obtained from (12).



Authorized licensed use limited to: Xian Jiaotong University. Downloaded on January 21,2021 at 09:30:29 UTC from IEEE Xplore. Restrictions apply.

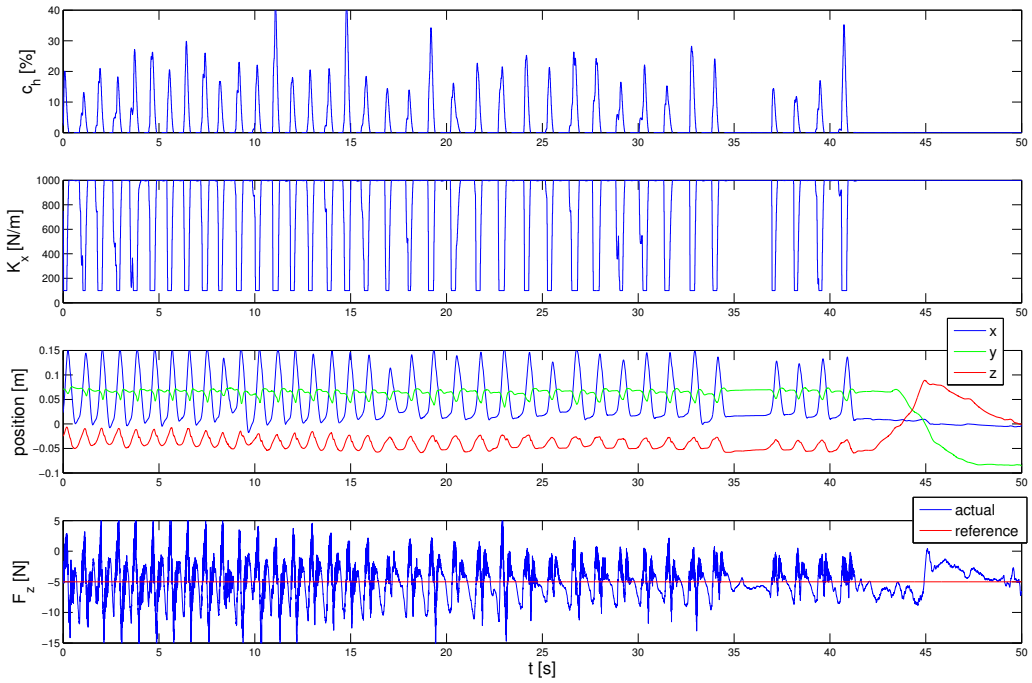


Fig. 2: Results of cooperative human-robot sawing using the proposed control approach. First graph shows the human stiffness estimation. Second graph depicts the robot stiffness along the sawing motion axis. Third graph presents the robot end-effector position along sawing axis (x), along beam axis (y) and along vertical axis (z). Finally, the fourth graph introduces the measured (blue) and reference (red) force along vertical axis.

saw teeth and the wood for the cutting. On average, the actual force was close to the desired. While there were deviations from the desired force due to the interaction with a very rough environment and due to some tilting during the practical execution, these non-ideal conditions did not affect the successful performance of the task.

One of the advantages of the proposed approach is its real-time adaptability. The human can arbitrary increase or decrease the frequency of task execution, or even stop the motion and then continue the motion at any point. The robot can estimate the intention of the human through the developed human-robot interface. The different execution frequency can be observed in the third graph, where the motion frequency was higher in 0-17 seconds section compared to 17-35 seconds section. The human temporary halted the task execution around 35 seconds and continued it a couple of seconds later. At the end, a new cut was made at different position along the beam. This can be observed by measured robot end-effector position in y-axis in the third graph.

In the second part of experiment we demonstrated the adaptability of the proposed approach, while varying the orientation of the main cutting motion, using the proposed task-frame feedback interface based on the force manipulability ellipsoid of the human arm end-point. We employed an optical motion capture system (OptiTrack) to measure the kinematics of the human arm and estimate its Jacobian matrix in real-time [29], [34]. Three optical markers mounted on a flat support base were placed on shoulder, elbow and wrist joints (7 DoF). We used the estimated human Jacobian to control the robot task frame orientation (stiffness) by (12). The estimated orientation was also used to align robotic hand orientation with human hand orientation. In the first stage, the subject was instructed to saw the beam of wood in an orientation aligned with x-axis of the robot base frame. In the second stage, the subject was instructed to change the configuration of the task frame so that the sawing was done in an axis that was rotated by approximately 45°. This was done continuously without stopping the setup. Please refer to supplementary multimedia file for a video of the experiment.

The results of this experiment are shown in Fig. 3. The photo and graphs on the left side correspond to the configuration when the task frame was aligned with the robot base frame, while the photo and graphs on the right side correspond to the rotated configuration. First four graphs correspond to the estimated human stiffness $c_h$, robot stiffness $K$ in x and y-axis of the robot base frame, rotation $\Theta$ of the task frame around vertical (z) axis and robot motion along task frame x-axis (sawing axis), respectively. Each graph shows one periodic cycle of the task. The graphs in the last row show the robot end-effector stiffness ellipsoid[5] in frame rotated by 180° along z-axis with respect to the robot base frame. We present it in this frame for the sake of more evident rotation with respect to the human on the photos. The black dotted lines in the second graph show when each of the stiffness ellipsoid was sampled.

By observing the human stiffness and robot stiffness we can see how the cooperating agents exchanged the pulling and following phases with respect to the motion of the blade. When the blade motion reached the desired peak while the human was pulling, the robot stiffness began to increase and drove the saw back toward itself. Similarly, when the

[5]Since the stiffness in axis perpendicular to sawing motion axis was set to zero, the ellipsoid naturally collapsed into a line in this case. For the sake of generality we still use the term "ellipsoid".



Authorized licensed use limited to: Xian Jiaotong University. Downloaded on January 21,2021 at 09:30:29 UTC from IEEE Xplore. Restrictions apply.

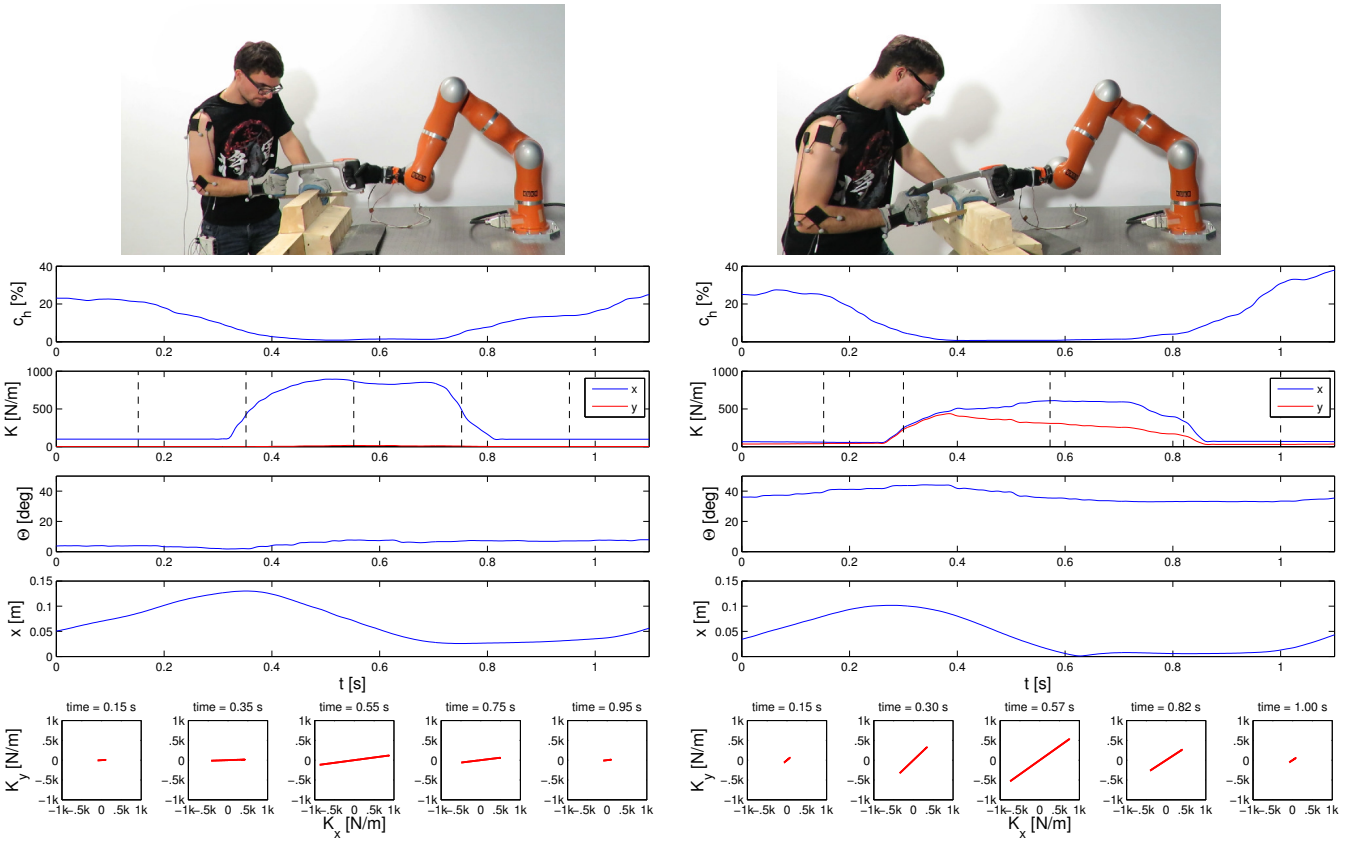


(a) Task frame aligned with the robot base frame

(b) Task frame rotated with respect to the robot base frame

Fig. 3: Result of experiment when using human force manipulability based task-frame configuration interface. The two photos show different configurations of the task frame. Graphs on the left side correspond to configuration where sawing axis of task frame was aligned with robot base frame x-axis, while graphs on the left side correspond to configuration where sawing axis of task frame was rotated with respect to the robot base frame. The last row graphs show robot stiffness ellipsoids at different phase of the periodic cycle. The black lines in second graphs indicate the moments when they were sampled.

blade motion reached the opposite peak, the human started to pull the saw and the robot became compliant. The stiffness dropped to the prescribed $k_{min}$, which was used to emulate the passive stiffness of the human muscles.

In the first stage, the task frame was aligned with the robot base frame, therefore stiffness in y-axis of the robot base frame was zero. This allowed the human to freely move the saw along the beam of wood to arbitrary choose the desired cutting location. When the wood beam was rotated, a new desired configuration of the task frame was required and the human intuitively adjusted it through the configuration interface. This can be confirmed by observing different angles $\Theta$ in left and right graphs. The same can be confirmed by the comparison between the graphs of stiffness ellipsoid, where we can also see how the sawing axis of the ellipsoid scaled with the human stiffness estimation $c_h$ according to (8).

## IV. Discussion

In this paper we present a novel multi-modal interface and control method for human-robot collaborative tasks. The main advantage of the proposed method is that it does not necessary require robot learning or complex pre-programming. Instead it relies on the developed real-time feedback interfaces and minimal degree of pre-programming. Despite this, the setup can achieve relatively good adaptability and intuitiveness. For example, the frequency of the task execution can be controlled directly by the human and the execution can be arbitrary halted and restarted. This is an advantage compared to more complex setup that uses adaptive oscillators to periodically repeat the learnt trajectories [6].

The myoelectric feedback interface within the proposed framework alone can provide a decent tool for human-robot cooperation in some co-manipulative tasks. The applicability of the proposed method is further increased by the recent development of affordable and easy-to-use EMG systems. While the exact estimation of the human impedance and motor behaviour requires measurement of multiple muscles in the arm [4], it has been shown that simplified estimations based on measurement of fewer muscles can provide sufficient practical results [6], [29]. However, in simplified estimations, different muscles might be considered for the myoelectric feedback interface in different tasks.

If additional complexity is affordable, the proposed task-frame configuration feedback interface can be integrated into the framework to provide extended adaptability. In addition, the motion capture system can be then also utilised to provide real-time visual feedback for controlling the desired robot trajectories [16], [23]. Alternatively, robot learning can



Authorized licensed use limited to: Xian Jiaotong University. Downloaded on January 21,2021 at 09:30:29 UTC from IEEE Xplore. Restrictions apply.

be employed to obtain the reference trajectories for more complex tasks [5]–[9], [27].

In future we will focus on developing and including other modalities into the proposed human-robot collaboration framework, such as visual feedback and robot learning, to be able to deal with the most complex tasks. In addition, we will use the proposed framework to solve other tasks, such as cooperative valve/bolt turning that was briefly mentioned in section II-B.2.

## ACKNOWLEDGMENT

The authors would like to thank Cheng Fang for providing algorithm for human arm Jacobian calculation.

## REFERENCES

[1] N. Hogan, "Impedance control - An approach to manipulation. I - Theory. II - Implementation. III - Applications," *ASME Transactions Journal of Dynamic Systems and Measurement Control B*, vol. 107, pp. 1–24, Mar. 1985.

[2] A. Albu-Schäffer, C. Ott, and G. Hirzinger, "A unified passivity-based control framework for position, torque and impedance control of flexible joint robots," *Int. J. Rob. Res.*, vol. 26, no. 1, pp. 23–39, Jan. 2007.

[3] C. Yang, G. Ganesh, S. Haddadin, S. Parusel, A. Albu-Schäffer, and E. Burdet, "Human-like adaptation of force and impedance in stable and unstable interactions," *Robotics, IEEE Transactions on*, vol. 27, no. 5, pp. 918–930, Oct 2011.

[4] A. Ajoudani, *Transferring Human Impedance Regulation Skills to Robots*. Springer, 2016.

[5] A. Gams, B. Nemec, A. Ijspeert, and A. Ude, "Coupling movement primitives: Interaction with the environment and bimanual tasks," *Robotics, IEEE Transactions on*, vol. 30, no. 4, pp. 816–830, Aug 2014.

[6] L. Peternel, T. Petrič, E. Oztop, and J. Babič, "Teaching robots to cooperate with humans in dynamic manipulation tasks based on multi-modal human-in-the-loop approach," *Autonomous robots*, vol. 36, no. 1-2, pp. 123–136, Jan 2014.

[7] L. Peternel, T. Petrič, and J. Babič, "Human-in-the-loop approach for teaching robot assembly tasks using impedance control interface," in *Robotics and Automation (ICRA), 2015 IEEE International Conference on*, May 2015, pp. 1497–1502.

[8] L. Rozo, D. Bruno, S. Calinon, and D. G. Caldwell, "Learning optimal controllers in human-robot cooperative transportation tasks with position and force constraints," in *Intelligent Robots and Systems (IROS), 2015 IEEE/RSJ International Conference on*, 2015.

[9] A. Ureche, K. Umezawa, Y. Nakamura, and A. Billard, "Task parameterization using continuous constraints extracted from human demonstrations," *Robotics, IEEE Transactions on*, vol. 31, no. 6, pp. 1458–1471, Dec 2015.

[10] C. Schindlbeck and S. Haddadin, "Unified passivity-based cartesian force/impedance control for rigid and flexible joint robots via task-energy tanks," in *Robotics and Automation (ICRA), 2015 IEEE International Conference on*, May 2015, pp. 440–447.

[11] R. Ikeura and H. Inooka, "Variable impedance control of a robot for cooperation with a human," in *Robotics and Automation (ICRA), 1995 IEEE International Conference on*, vol. 3, May 1995, pp. 3097–3102.

[12] K. Kosuge and N. Kazamura, "Control of a robot handling an object in cooperation with a human," in *Robot and Human Communication, 6th IEEE International Workshop on*, Sep 1997, pp. 142–147.

[13] O. Al-Jarrah and Y. Zheng, "Arm-manipulator coordination for load sharing using reflexive motion control," in *Robotics and Automation (ICRA), 1997 IEEE International Conference on*, vol. 3, Apr 1997, pp. 2326–2331.

[14] T. Tsumugiwa, R. Yokogawa, and K. Hara, "Variable impedance control with virtual stiffness for human-robot cooperative peg-in-hole task," in *Intelligent Robots and Systems (IROS), 2002 IEEE/RSJ International Conference on*, vol. 2, 2002, pp. 1075–1081.

[15] V. Duchaine and C. Gosselin, "General model of human-robot cooperation using a novel velocity based variable impedance control," in *Eurohaptics Conference and Symposium on Haptic Interfaces for Virtual Environment and Teleoperator Systems, 2rd Joint*, March 2007, pp. 446–451.

[16] D. Agravante, A. Cherubini, A. Bussy, P. Gergondet, and A. Kheddar, "Collaborative human-humanoid carrying using vision and haptic sensing," in *Robotics and Automation (ICRA), 2014 IEEE International Conference on*, May 2014, pp. 607–612.

[17] E. Gribovskaya, A. Kheddar, and A. Billard, "Motion learning and adaptive impedance for robot control during physical interaction with humans," in *Robotics and Automation (ICRA), 2011 IEEE International Conference on*, May 2011, pp. 4326–4332.

[18] P. Evrard, E. Gribovskaya, S. Calinon, A. Billard, and A. Kheddar, "Teaching physical collaborative tasks: object-lifting case study with a humanoid," in *IEEE-RAS International Conference on Humanoid Robots*, 2009, pp. 399–404.

[19] P. Donner, A. Mortl, S. Hirche, and M. Buss, "Human-robot cooperative object swinging," in *Robotics and Automation (ICRA), 2013 IEEE International Conference on*, May 2013, pp. 4343–4349.

[20] I. Palunko, P. Donner, M. Buss, and S. Hirche, "Cooperative suspended object manipulation using reinforcement learning and energy-based control," in *Intelligent Robots and Systems (IROS), 2014 IEEE/RSJ International Conference on*, Sept 2014, pp. 885–891.

[21] S. Ikemoto, H. Ben Amor, T. Minato, B. Jung, and H. Ishiguro, "Physical human-robot interaction: Mutual learning and adaptation," *Robotics Automation Magazine, IEEE*, vol. 19, no. 4, pp. 24 –35, Dec 2012.

[22] L. Peternel and J. Babič, "Learning of compliant human-robot interaction using full-body haptic interface," *Advanced Robotics*, vol. 27, no. 13, pp. 1003–1012, Jun 2013.

[23] A. De Santis, V. Lippiello, B. Siciliano, and L. Villani, "Human-robot interaction control using force and vision," in *Advances in Control Theory and Applications*, C. Bonivento, L. Marconi, C. Rossi, and A. Isidori, Eds., 2007, vol. 353, pp. 51–70.

[24] J. Medina, M. Shelley, D. Lee, W. Takano, and S. Hirche, "Towards interactive physical robotic assistance: Parameterizing motion primitives through natural language," in *RO-MAN, 2012 IEEE*, Sept 2012, pp. 1097–1102.

[25] L. Peternel, T. Noda, T. Petrič, A. Ude, J. Morimoto, and J. Babič, "Adaptive control of exoskeleton robots for periodic assistive behaviours based on EMG feedback minimisation," *PLoS ONE*, vol. 11, no. 2, p. e0148942, Feb 2016.

[26] M. Lawitzky, J. Medina, D. Lee, and S. Hirche, "Feedback motion planning and learning from demonstration in physical robotic assistance: differences and synergies," in *Intelligent Robots and Systems (IROS), 2012 IEEE/RSJ International Conference on*, Oct 2012, pp. 3646–3652.

[27] M. Ewerton, G. Neumann, R. Lioutikov, H. B. Amor, J. Peters, and G. Maeda, "Learning multiple collaborative tasks with a mixture of interaction primitives," in *Robotics and Automation (ICRA), 2015 IEEE International Conference on*, May 2015, pp. 1535–1542.

[28] K. B. Reed and M. A. Peshkin, "Physical collaboration of human-human and human-robot teams," *Haptics, IEEE Transactions on*, vol. 1, no. 2, pp. 108–120, 2008.

[29] A. Ajoudani, C. Fang, N. G. Tsagarakis, and A. Bicchi, "A reduced-complexity description of arm endpoint stiffness with applications to teleimpedance control," in *Intelligent Robots and Systems (IROS), 2015 IEEE/RSJ International Conference on*, Sept 2015, pp. 1017–1023.

[30] A. Ajoudani, S. Godfrey, M. Bianchi, M. Catalano, G. Grioli, N. Tsagarakis, and A. Bicchi, "Exploring teleimpedance and tactile feedback for intuitive control of the pisa/iit softhand," *Haptics, IEEE Transactions on*, vol. 7, no. 2, pp. 203–215, April 2014.

[31] M. Ison and P. Artemiadis, "The role of muscle synergies in myoelectric control: trends and challenges for simultaneous multifunction control," *Journal of neural engineering*, vol. 11, no. 5, p. 051001, 2014.

[32] M. Turvey, "Action and perception at the level of synergies," *Human Movement Science*, vol. 26, no. 4, pp. 657–697, 2007.

[33] A. Albu-Schäffer, C. Ott, U. Frese, and G. Hirzinger, "Cartesian impedance control of redundant robots: recent results with the DLR-light-weight-arms," in *Robotics and Automation (ICRA), 2003 IEEE International Conference on*, vol. 3, Sept 2003, pp. 3704–3709.

[34] X. Ding and C. Fang, "A novel method of motion planning for an anthropomorphic arm based on movement primitives," *IEEE/ASME Transactions on Mechatronics*, vol. 18, no. 2, pp. 624–636, April 2013.



Authorized licensed use limited to: Xian Jiaotong University. Downloaded on January 21,2021 at 09:30:29 UTC from IEEE Xplore. Restrictions apply.